WATER RESOURCES RESEARCH, VOL. 31, NO. 6, PAGES 1533–1541, JUNE 1995

Similarity in catchment response 1. Stationary rainstorms

Bahram Saghafian and Pierre Y. Julien
Civil Engineering Department, Colorado State University, Fort Collins

Fred L. Ogden[1]
Department of Civil Engineering, University of Connecticut, Storrs

Abstract. The variability in Hortonian surface runoff discharge and volume produced by stationary rainstorms on watersheds with spatially distributed soil saturated hydraulic conductivity is examined using a two-dimensional runoff model and a Monte Carlo methodology. Results indicate that rainfall duration t_r, rainfall intensity i, representative time to equilibrium t_{re}, mean saturated hydraulic conductivity K_m, and coefficient of variation C_v play major roles in the variability of surface runoff. Similarity in surface runoff generated on heterogeneous soils is governed by the following dimensionless parameters: $T^* = t_r/t_{re}$, $K^* = K_m/i$, and C_v. The variability in both discharge and runoff volume for randomly distributed systems increases with K^* and C_v, compared to the runoff generated from uniformly distributed systems. Runoff variability decreases when T^* increases unless the mean value of hydraulic conductivity approaches the rainfall intensity ($K^* \rightarrow 1$). In highly pervious watersheds the steady state discharge depends on the spatial distribution of hydraulic conductivity. Lumped values of saturated hydraulic conductivity are found to typically underestimate the peak discharge and runoff volume.

1. Introduction

1.1. Previous Work

Natural watersheds exhibit spatial heterogeneity in topography, surface roughness, vegetation, and soil infiltration characteristics. Several investigations have examined the influence of the spatial variability of these factors on runoff. For example, effects of random distribution of infiltration characteristics were explored by *Smith and Hebbert* [1979] using a Monte Carlo simulation of soil infiltration properties. The mean ponding time in a composite simulation showed little bias. However, the mean infiltration rate was particularly biased at greater coefficients of variation and smaller ratios of rainfall intensity to saturated hydraulic conductivity. In an interactive watershed simulation run on a surface with 400 representative points of varying infiltration, randomization at higher rainfall rates showed very little effect as compared with uniformly infiltrating surface.

Freeze [1980] used a stochastic-conceptual hydrologic model to investigate the influence of spatial stochastic properties of hillslope parameters on the statistical properties of runoff events. Both Hortonian and Dunne overland flow generation mechanisms were simulated. The results ranked the importance of the stochastic properties of the distribution of hydraulic conductivity as follows: the mean value, the standard deviation, and the autocorrelation function. Freeze warned that great error may be introduced in the statistics of predicted runoff when an equivalent uniform hillslope is used in lieu of a heterogeneous hillslope, for a sequence of stochastically generated storm events.

Milly and Eagleson [1982] treated a heterogeneous soil surface as a battery of independent soil columns to calculate the areal average infiltration rate resulting from a spatially varied storm event. Their study revealed that spatial variability in soil type and rainfall depth typically leads to decreased cumulative infiltration and increased surface runoff. The sensitivity of cumulative infiltrated depth to the initial soil moisture conditions was greatest for basins with shallow soils or high water tables. In later work, *Milly and Eagleson* [1988] studied the effects of storm size on surface runoff volume. They used a simple conceptual model of surface runoff in conjunction with derived expressions for the areal average surface runoff. The derivation depended on the description of large-scale variation of the storm depth-duration relationship. It was concluded that contrary to runoff from saturated or impervious source areas, the infiltration excess runoff volume is extremely sensitive to the storm size. Furthermore, it was stated that spatial variability of precipitation generally increases surface runoff compared to uniform rainfall.

Assuming no run-on and using an approximate model for point rainfall infiltration based primarily on Philip's equation combined with a time compression approximation (TCA), *Sivapalan and Wood* [1986] derived quasi-analytical expressions for the statistics of ponding time and infiltration rate for two cases: spatially varied soils with uniform rainfall; and uniform soil properties with spatially varied rainfall. Similar to the results of *Smith and Hebbert* [1979], considerable differences in infiltration rate arose when using average soil properties as opposed to spatially varied soil characteristics. Additionally, it was suggested that rainfall spatial variability was more critical than soil characteristic spatial variability in modeling the rainfall-runoff response.

[1]Formerly at Civil Engineering Department, Colorado State University, Fort Collins.

Paper number 95WR00518.
0043-1397/95/95WR-00518$05.00

Using a simple model describing infiltration and unsteady flow over a plane and a single channel, *Woolhiser and Goodrich* [1988] investigated the sensitivity of runoff volume and peak flow due to different rainfall disaggregation methods and to the spatial variability of infiltration parameters. In their analysis the effective saturated hydraulic conductivity was lognormally distributed over five parallel strips with widths equal to one fifth of the width of each plane of an open-book geometry. As a major improvement over models dealing only with point statistics and runoff volume quantities, flow routing was also performed for overland flow and channel flow using the one-dimensional kinematic wave technique. *Woolhiser and Goodrich* [1988] found that a uniform plane represented by the geometric mean of hydraulic conductivity yielded higher peak discharges for low infiltration rates or high-intensity storms. They also found that spatially varied infiltration generated higher peaks for larger geometric mean infiltration rates given low to medium rainfall rates. For the elementary watershed considered, the channel characteristics showed no effect on the overall basin response in comparison to overland flow characteristics.

Spatial variability in slope, roughness, width, and excess rainfall on a one-dimensional runoff plane was examined by *Julien and Moglen* [1990]. Results from 8400 simulated dimensionless hydrographs under spatially varied input indicated that variability in discharge from impervious surfaces depends primarily on the ratio of rainfall duration to the time to equilibrium. Outflow variability defined in terms of the relative sensitivity from all four spatially varied parameters, uncorrelated and correlated, decreased in a similar manner with increasing rainfall duration. Spatially varied excess rainfall demonstrated the greatest relative sensitivity effect, while slope had the least effect.

Spatially varied rainfall over small impervious watersheds was examined by *Ogden and Julien* [1993] using two-dimensional simulations with the CASC2D rainfall-runoff model. The relative sensitivity of runoff to spatially varied rainfall was found to decrease with increasing rainfall duration, identically to the one-dimensional results reported by *Julien and Moglen* [1990].

The study reported herein emphasizes the interaction of rainfall, infiltration, surface routing, and run-on processes which ultimately produce an integrated response in the form of a discharge hydrograph at the outlet. As such, this work differs from previous studies by *Sivapalan and Wood* [1986], *Milly and Eagleson* [1982, 1988], and the first part of the work by *Smith and Hebbert* [1979], who mainly focused on the composite simulation of point response. Although different in the scale of the watershed selected, this effort is similar to those of *Freeze* [1980] and *Woolhiser and Goodrich* [1988] in employing interactive watershed simulation techniques. Also analogous to these latter studies, we define the spatially variable watershed parameter by a set of stochastic processes. However, the choice of our research tool, i.e. the rainfall-runoff model, is different from the others and allows full two-dimensional surface runoff routing and simulation of run-on process. It is demonstrated that run-on can have a pronounced effect on both the discharge and the volume of runoff even for saturated watersheds. The type and range of the introduced governing variables in this study differ from the cited literature. Nevertheless, some of the conclusions concur with others, and some are specific to this study. While some studies have included saturation-excess runoff as well [*Freeze* 1980], this work is limited to infiltration-excess only.

1.2. Objectives

The objectives of this study are to (1) introduce governing variables which characterize the effect of spatially varied infiltration on the peak discharge and runoff volume from two-dimensional watersheds subject to stationary uniform storms; (2) ascertain the effect of rainfall duration on the sensitivity of a catchment to spatially varied saturated hydraulic conductivity; (3) relate the magnitude of watershed sensitivity to spatially varied infiltration to the coefficient of variation of the hydraulic conductivity distribution; (4) search for possible bias in the application of average soil properties in lieu of distributed systems; (5) examine the sensitivity of initial soil moisture on the magnitude of surface runoff for spatially varied infiltration; and (6) investigate similarity between distributed soils and rainfall. The results are presented in dimensionless form, over an expected range of natural rainfall and watershed conditions, to promote the applicability of these results to other watersheds.

2. General Description and Methodology

2.1. Model Description

A two-dimensional hydrodynamic rainfall-runoff model, CASC2D, was used to simulate catchment response in this study. The primary features of CASC2D include the Green and Ampt infiltration, two-dimensional finite difference (FD) diffusive wave overland flow routing, and one-dimensional FD diffusive wave channel routing. Watershed topography and soil characteristics are represented using raster (square grid) cells. Although spatial variability is allowed from one grid cell to the next, each cell is represented as a homogeneous unit.

The Green-Ampt equation is used to determine Hortonian infiltration losses. Assuming a homogeneous, deep, and well-drained soil [*Rawls et al.*, 1983],

$$f = K\left(1 + \frac{H_f M_d}{F}\right) \tag{1}$$

where f is the infiltration rate; K is the saturated hydraulic conductivity; H_f is the capillary pressure head at the wetting front; M_d is the soil moisture deficit, equal to $(\theta_e - \theta_i)$; θ_e is the effective porosity, equal to $(\phi - \theta_r)$; ϕ is the total porosity; θ_r is the residual saturation; θ_i is the initial moisture content; and F is the total infiltrated depth. The degree of initial soil saturation S in percent is given by $S = 100\ \theta_i/\theta_e$. The excess head due to surface water depth is neglected as being small compared to the capillary pressure head H_f. The actual infiltration rate is taken as the lesser of the infiltration capacity and the maximum available rate controlled by the ponded surface water depth, to which the incremental rainfall depth has been added. There is no provision for the recovery of infiltration capacity due to soil moisture redistribution between storms in the version of CASC2D used in this study, which does not significantly affect single-storm simulations.

The Saint-Venant equations of continuity and momentum describe the mechanics of gradually varied overland flow. The two-dimensional continuity equation in partial differential form reads

$$\frac{\partial h}{\partial t} + \frac{\partial q_x}{\partial x} + \frac{\partial q_y}{\partial y} = i_e \tag{2}$$

where h is the surface flow depth; q_x is the unit discharge in the x direction; q_y is the unit discharge in the y direction; i_e is the excess rainfall, equal to $(i - f)$; i is the rainfall intensity; x and y are rectangular coordinates; and t is time. The momentum equations in the x and y directions may be derived by relating the net forces per unit mass to flow acceleration. The diffusive wave approximation of the momentum equation in the x direction, for instance, is

$$S_{fx} = S_{0x} - \frac{\partial h}{\partial x} \tag{3}$$

where S_{fx} is the friction slope; and S_{0x} is the bed slope. Both slopes are in the x direction.

A resistance law, in terms of the depth-discharge relationship, is required for the solution of the above set of differential equations. Such a relation may be expressed as

$$q_x = \alpha_x h^{\beta} \tag{4}$$

where α_x varies with the derivative of depth in the diffusive wave formulation and β is a constant. Both α_x and β depend upon flow regime, i.e., laminar or turbulent. In the case of turbulent flow over a rough boundary, the Manning resistance equation, in SI units, may be used:

$$\alpha_x = S_{fx}^{1/2}/n \qquad \beta = \tfrac{5}{3} \tag{5}$$

where n is the Manning roughness coefficient. Notice that while β remains constant, α_x varies during a rainstorm simulation according to S_{fx}.

Finite width channel flow routing is performed similarly to overland flow routing but in a single direction along the channel path. Accordingly, the one-dimensional continuity equation for channel flow replaces (2), whereas (3) still represents the simplified momentum equation. The overland flow and channel flow are fully coupled, allowing lateral inflow and outflow from the channels. The model also enables simulation of run-on and subsequent reinfiltration, which occurs when surface runoff from upstream cells infiltrates in pervious downstream cells.

CASC2D is fully documented by *Julien and Saghafian* [1991] and was verified on a number of watersheds in Mississippi by *Johnson et al.* [1993]. A number of other studies have also employed this model as a research tool [e.g., *Ogden and Julien*, 1993, 1994; *Doe and Saghafian*, 1992].

2.2. Methodology

The semiarid Macks Creek experimental watershed [*Robins et al.*, 1965] was selected for use in this study. Macks Creek is a 32.2-km^2 subbasin of the Reynolds Creek Experimental Watershed in southwestern Idaho. This catchment is quite steep, with an elevation drop of 750 m in 8 km. Overland plane slopes approach 30% in portions of the basin. Two main channels with slopes averaging 5% and lengths near 10 km collect surface runoff. The topography of the watershed is depicted in Figure 1.

The response of Macks Creek as simulated by CASC2D was analyzed in terms of peak discharge and runoff volume. A Monte Carlo methodology was employed to generate spatial distributions of hydraulic conductivity. Each Monte Carlo ensemble consisted of 50 spatially uncorrelated simulations with

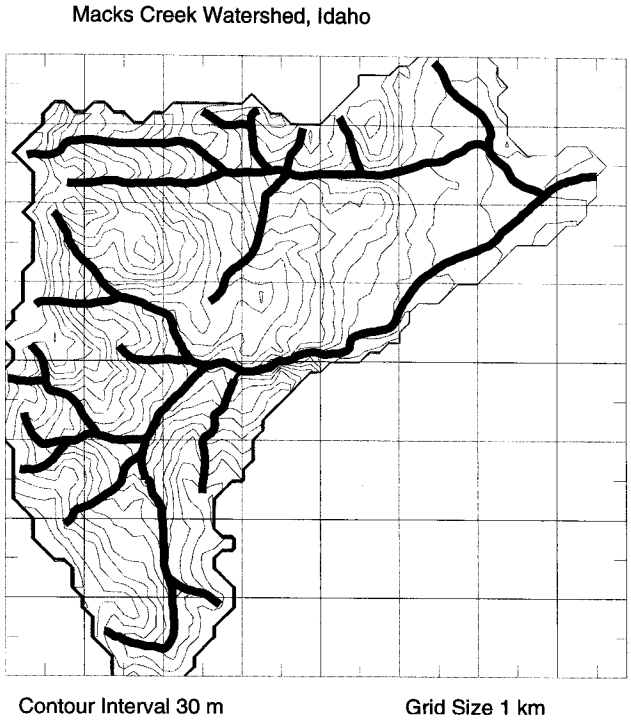

Figure 1. Topography of Macks Creek watershed.

identical statistical properties. A sensitivity analysis showed that an ensemble size of 100 simulations produced little change in simulated outflow statistics over 50 simulations. In light of the reduced computational effort, a soil (raster) grid size of 600 m was used. Spatial correlation of hydraulic conductivity at this scale was ignored since this grid size is significantly larger than the correlation length of hydraulic conductivity [*Loague and Gander*, 1990]. The assumption is made that soil properties are uniform within the individual grid cells at the selected grid size.

Hydraulic conductivity values are typically lognormally distributed in space [*Nielsen et al.*, 1973; *Sharma et al.*, 1987]. Assuming a lognormal distribution, selected values of arithmetic mean hydraulic conductivity K_m and coefficient of variation C_v were used to generate discrete values of hydraulic conductivity at each grid cell of Macks Creek watershed.

The CASC2D rainfall-runoff model was used to calculate the surface runoff from each of the 50 different realizations of spatially varied hydraulic conductivity under various storm and soil conditions. With more than 20,000 simulations required for the completion of this study, computational efficiency was of the essence. Thus as one simplifying assumption, no incised channel routing was performed. All surface flow over the entire watershed was routed as overland flow; i.e., the channel cross sections were assumed to be wide, pervious, and subject to spatial variability. Although this may limit the applicability of the results to overland-dominated watersheds, until further analysis is performed, the effect of such treatment is reflected in prolonged watershed response time t_{re} (see section 2.3) and thus carried through the entire analysis.

Macks Creek is predominantly covered by loamy soils; thus the values of mean hydraulic conductivity K_m, capillary head H_f, and effective porosity θ_e used were 3.6 cm/h (1×10^{-6} m/s), 8.89 cm, and 0.434 cm^3/cm^3, respectively [*Rawls et al.*, 1983]. The coefficient of variation of hydraulic conductivity C_v was systematically varied to reflect an appropriate range of C_v

Table 1. Values of Rainfall Intensity i, Equivalent Equilibrium Time t_e, Equivalent Ponding Time t_p, and Representative Equilibrium Time t_{re}

	$K^* = 0.1$	$K^* = 0.2$	$K^* = 0.4$	$K^* = 0.6$	$K^* = 0.8$
$i \times 10^6$, m/s	10.0	5.0	2.5	1.667	1.25
t_e, min	185	256	379	524	776
t_p for $S = 10\%$, min	6	29	154	521	1,852
t_p for $S = 50\%$, min	4	16	86	289	1,029
t_p for $S = 100\%$, min	0	0	0	0	0
t_{re} for $S = 10\%$, min	191	285	533	1,045	2,628
t_{re} for $S = 50\%$, min	188	272	465	813	1,805
t_{re} for $S = 100\%$, min	185	256	379	524	776

values. *Sharma et al.* [1980] and *Loague and Gander* [1990], respectively, suggested values of C_v in the range of 0.6 to 0.7 for steady state infiltration rates across the R-5 Watershed in Oklahoma covering an area of 0.1 km^2. Spatial variability is expected to increase on larger watersheds, so three different C_v values were tested in this study: 0.5, 1, and 2. Three values of initial saturation S (10%, 50%, and 100%), representing dry, moist, and saturated conditions were tested in a systematic fashion. Both H_f and S were assumed spatially uniform.

2.3. Governing Variables

Up to this point we have only introduced one of our selected dimensionless variables: C_v is used as a measure of the spatial variability of saturated hydraulic conductivity over the watershed. Here we introduce two more governing variables, which collectively integrate the effect of rainfall and other watershed characteristics. These variables are a dimensionless time variable T^* and a dimensionless infiltration rate variable K_r^* described below.

First we turn our attention to the temporal variable. Specifically, the duration of rainfall (t_r) and the time to representative equilibrium (t_{re}) are used to describe the temporal nature of the rainfall and the temporal response of the catchment to a particular rainfall rate. While the variable t_r defines the duration of rainfall, there is no simple and readily apparent temporal response parameter for pervious watersheds. We propose taking the kinematic time to equilibrium t_e for an impervious watershed and adding the ponding time t_p for the mean pervious system to encapsulate the complexity of watersheds with temporally varying infiltration. The resultant time is defined as the representative equilibrium time for the watershed (t_{re}).

We normalize the time characteristic of the rainstorm with the temporal response of the watershed such that $T^* = t_r/t_{re}$. As shown later, the kinematic equilibrium time effectively embodies spatial scale and physiogeometrical characteristics of the watershed as well as storm intensity. The average ponding time brings in the effects of soil hydraulic properties and initial conditions. Thus

$$t_{re} = t_p + t_e \tag{6}$$

where $t_p = K_m H_f M_d/[i(i - K_m)]$ is the ponding time for the mean value of hydraulic conductivity computed from the Green-Ampt equation and t_e is the equilibrium time computed as the elapsed time for an impervious watershed to reach steady state under constant excess rainfall intensity of $(i - K_m)$.

The kinematic time to equilibrium t_e may be defined as the time at which watershed runoff discharge reaches steady state under a very long storm. For such a storm, time to equilibrium and time of concentration t_c are identical. Both are indicative of the watershed response time and inherently vary with storm intensity. Relationships for the kinematic time to equilibrium were analytically derived for well-defined simple geometries [*Lighthill and Whitham*, 1955; *Henderson and Wooding*, 1964; *Wooding*, 1965; *Agiralioglu*, 1984, 1988]. *Saghafian* [1992] derived an analytical relationship for t_e for complex watersheds subject to distributed rainfall. In this study, with spatially uniform rainfall, this relationship was applied, resulting in

$$t_e = \frac{1}{i^\gamma} \int_0^L (1 - \gamma) \left(\frac{a_1}{A}\right)^\gamma \left(\frac{n}{a_2^{2/3} S_0^{1/2}}\right)^{1-\gamma} dx \tag{7}$$

where $\gamma = 2b_2/(2b_2 + 3b_1)$; L is the length of the hydraulically longest trajectory terminating at the outlet; A is the local drainage (upslope) area; n is the local Manning roughness coefficient; S_0 is the local bed slope; and a_1, b_1, a_2, and b_2 are cross-sectional geometry coefficients in cross-section area $A_x = a_1 h^{b1}$ and hydraulic radius $R = a_2 h^{b2}$. The time to equilibrium t_e is computed by adding the travel time for overland flow and channel flow phases. For example, solving (7) for a uniform rectangular overland plane yields the following well-known formula:

$$(t_{e0})_{rec} = \frac{n^{3/5} L_{0v}^{3/5}}{i^{2/5} S_{0v}^{3/10}} \tag{8}$$

Using a comprehensive raster-based approach, tools were developed whereby the variations inside the integral in (7) are numerically evaluated for complex watersheds [*Saghafian*, 1992]. This numerical algorithm was used on Macks Creek for any given set of the variables T_r, rainfall excess $(i - K_m)$, and initial moisture content in determining T_{re} and thus T^*. For as wide a range as possible, values of T^* tested in this study were $T^* = 0.1, 0.2, 0.4, 0.7, 1, 1.5, 2, 3, 5$, and T_p^* where $T_p^* = t_p/t_{re}$. The case of $T^* = T_p^*$ examines whether runoff occurs when rainfall duration equals the ponding time of the mean system.

In developing the second governing variable of this study K^*, we scaled the mean hydraulic conductivity with the average intensity of the storm: $K^* = K_m/i$; K^* should be indicative of magnitude of infiltration rates relative to rainfall intensity. The following values of K^* were simulated in this study:

$$K^*: 0.1, 0.2, 0.4, 0.6, 0.8$$

All major parameter values tested are listed in Tables 1 and 2.

Table 2. Values of Rainfall Duration t_r

	T^*									
K^*	0.1	0.2	0.4	0.7	1	1.5	2	3	5	T_p^*
					S = 10%					
0.1	19	38	77	134	191	287	383	574	957	6
0.2	29	57	114	199	285	427	570	855	1,425	29
0.4	53	107	213	373	533	800	1,067	1,600	2,667	154
0.6	105	209	418	731	1,045	1,567	2,090	3,135	5,225	521
0.8	263	526	1,051	1,840	2,628	3,942	5,256	7,885	13,141	1,852
					S = 50%					
0.1	19	38	75	132	189	283	377	566	944	4
0.2	27	54	109	191	272	408	545	817	1,362	16
0.4	47	93	186	325	465	697	930	1,394	2,324	86
0.6	81	163	325	569	813	1,220	1,626	2,440	4,067	289
0.8	181	361	722	1,264	1,805	2,708	3,610	5,415	9,025	1,029
					S = 100%					
0.1	18	37	74	129	185	277	370	555	925	0
0.2	25	51	102	179	256	384	512	768	1,281	0
0.4	38	76	152	265	379	569	758	1,138	1,869	0
0.6	52	104	210	366	524	786	1,048	1,572	2,620	0
0.8	78	156	310	544	776	1,164	1,552	2,328	3,880	0

Values are in minutes.

3. Results

3.1. Distribution of Peak Discharge

For any simulation within an ensemble corresponding to certain values of K^*, S, C_v, and T^*, the peak surface runoff discharge Q_p was divided by the peak discharge Q_m produced by the spatially uniform mean hydraulic conductivity system (reference system) for the same values of K^*, S, and T^*. The resulting 50 dimensionless peak discharges were log transformed and ranked, producing the cumulative density functions (CDF) plotted in Figures 2a–2e for $S = 10\%$ and $C_v = 0.5$. In these figures the log-transformed ratio Q_p/Q_m (except when Q_m or Q_p equal zero) varies with K^* and T^*. While the figures correspond to $S = 10\%$ and $C_v = 0.5$, it is observed that in all cases the distribution of peak discharge becomes more uniform as T^* increases for any given K^*, or as K^* decreases for any given T^*. The latter observation demonstrates that the effect of spatially variable hydraulic conductivity on runoff becomes small as storm intensity increases, because K^* decreases. This is particularly true when the coefficient of variation is small.

Figure 2e reveals that peak runoff rates produced by spatially varied systems are different from those produced by the mean system at large K^* even for very long duration storms which are expected to generate near–steady state conditions. As explained later in the discussion of hydrograph envelopes, such a discrepancy in peak discharge can be attributed to the pronounced effect of run-on volume generated in the distributed watershed when the mean hydraulic conductivity is close to the rainfall intensity. Also, the nonuniform behavior in the peak discharge distribution is observed for short but intense rainstorms. The results for other values of C_v indicated, as one may expect, that increasing C_v intensified the nonuniformity in the distribution of the peak discharge.

The majority of the spatially varied hydraulic conductivity systems produced higher peak discharges compared to those from the mean system, particularly for higher values of K^*. For the range of values examined, the likelihood of lower peak discharge from spatially varied systems increases with decreasing K^* and/or T^* but did not exceed 50% in any case. This implies that spatial variability of K dominates the surface runoff generation for low-intensity storms by producing higher peaks compared to the uniform system. This trend appears to weaken for higher-intensity storms, although the spatially distributed system is more likely to produce a higher peak discharge than the uniform system. Additionally, some of the distributed systems produced runoff discharge; the runoff production of the mean system was put off as K^* increased until longer-duration storms were tested. This is apparent from missing curves corresponding to low values of T^* in Figures 2b–2e.

3.2. Distribution of Outflow Volume

The CDF of runoff volume was also analyzed and found to exhibit trends similar to those from the peak discharge distribution. The spatial variability of hydraulic conductivity exerted a greater influence on the runoff volume than on the peak discharge. For relatively low intensity and short duration storms (large K^* and small T^*), the runoff volume is extremely sensitive to the spatial distribution of hydraulic conductivity in the catchment, so that using the mean value of hydraulic conductivity will likely cause very large differences in volume yield. Again, the majority of the spatially varied systems produced larger outflow volumes compared to the mean system.

3.3. Hydrograph Envelopes

In the previous sections the sensitivity of the peak discharge and runoff volume to spatially varied infiltration was explored. However, to measure the time-integrated sensitivity of the entire outflow hydrograph to spatial variability, hydrograph envelopes are constructed, one for each set of 50 computed hydrographs. A hydrograph envelope is developed by recording the maximum and minimum observed discharge at each computational time step over the 50 simulations. The volume

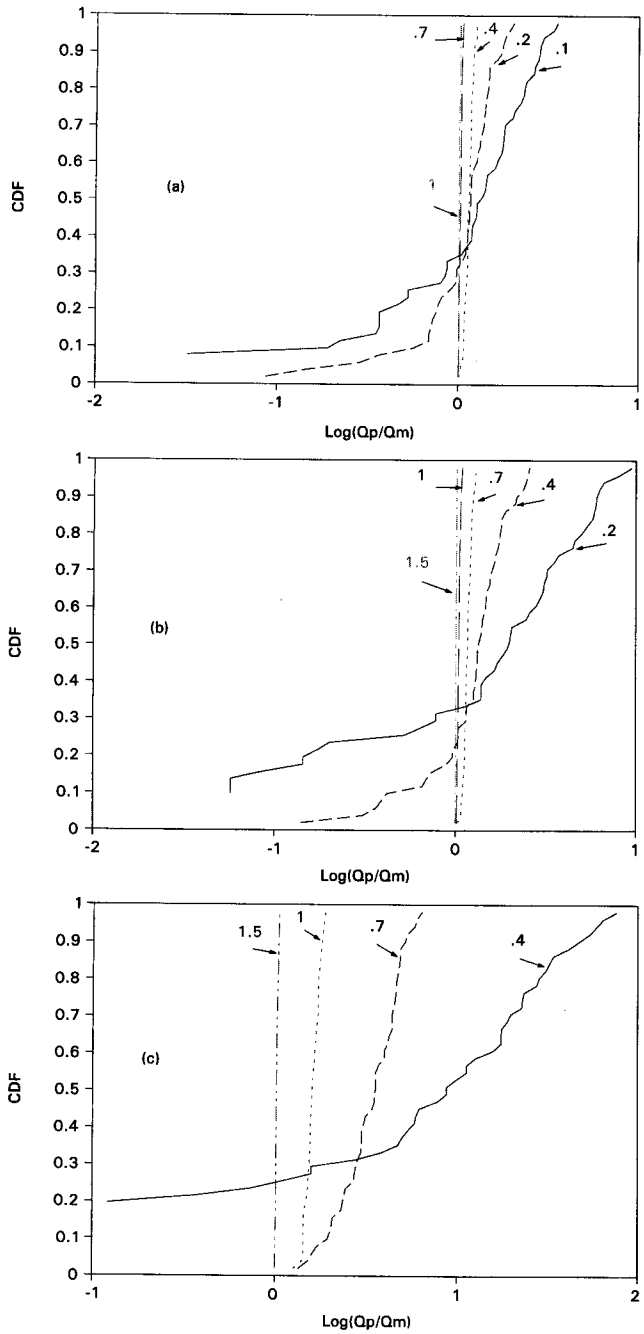

Figure 2. Peak discharge distribution with infiltration as a function of T^* for (a) $K^* = 0.1$, (b) $K^* = 0.2$, (c) $K^* = 0.4$, (d) $K^* = 0.6$, and (e) $K^* = 0.8$.

of runoff contained within the upper and lower bounds of the hydrograph envelope is indicative of runoff sensitivity to a given parameter variation. Examples of hydrograph envelopes are shown by *Julien and Moglen* [1990] and *Ogden and Julien* [1993].

The time-integrated volume of the hydrograph envelope ΔV is normalized with the mean volume of input excess rainfall to obtain the normalized hydrograph envelope volume V^*:

$$V^* = \frac{\Delta V}{(i - K_m)At_r} \tag{9}$$

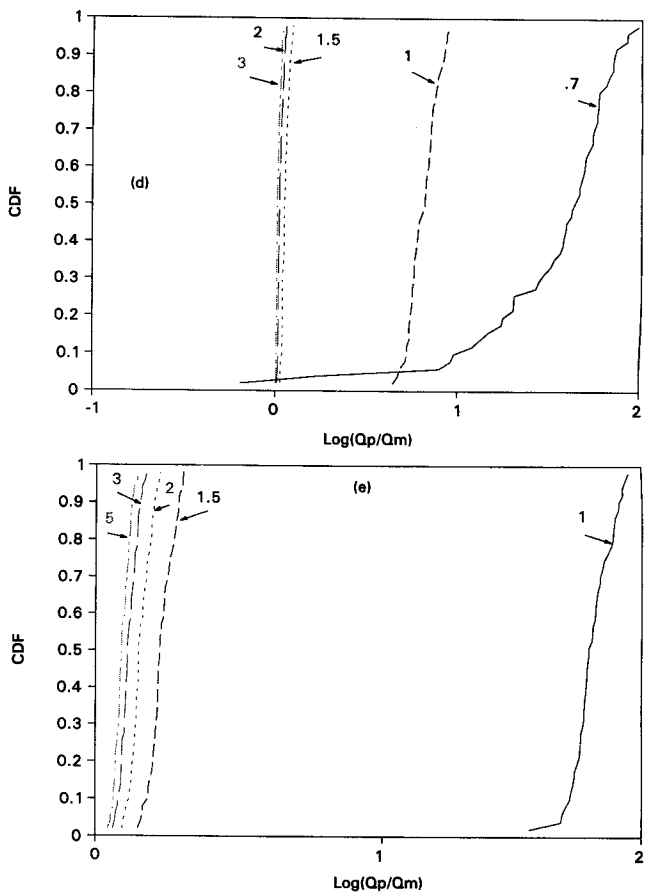

Figure 2. (continued)

where the numerator represents the volume within the hydrograph envelope and the denominator is the mean volume of steady state excess rainfall. The parameter A represents the total watershed area.

The variation of V^* versus T^* is plotted in Figure 3 for $S = 10\%$ and $C_v = 0.5$ for various values of K^*. As T^* increases, V^* rises rather steeply and either reaches a peak for smaller values of K^* or flattens for larger values of K^*. Both the magnitude and location of the peak generally increase with K^*. For $K^* = 0.8$, V^* approaches a constant value for large T^*, which indicates the volume under the hydrograph enve-

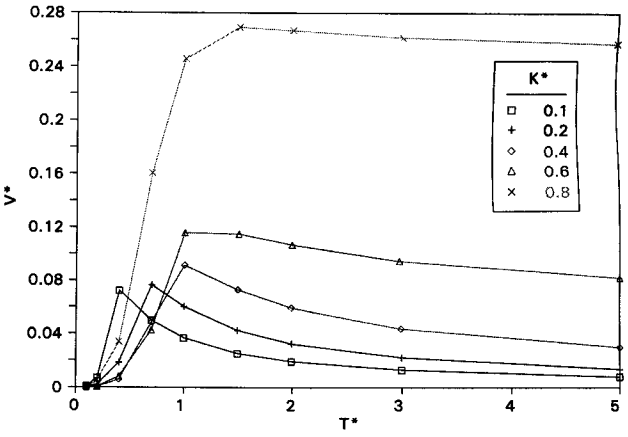

Figure 3. V^* versus T^* for pervious watersheds.

lope increases consistently with the excess rainfall volume under virtual steady state conditions, even when a larger $T^* = 10$ was examined to push the system to a closer equilibrium condition. When K^* is large, the infiltration capacity exceeds the rainfall rate over a large portion of the watershed, while surface runoff is generated in localized regions of reduced hydraulic conductivity. The runoff generated from an upstream cell flowing downstream as run-on may very well infiltrate over a cell with higher hydraulic conductivity. On the other hand, if lower values of hydraulic conductivity are placed near the outlet, surface runoff may reach the outlet and produce an outflow hydrograph. The placement of regions with relatively high hydraulic conductivity determines the run-on volume produced, which translates into differences in peak discharge at the virtual steady state. Dominantly increasing or decreasing trends in hydraulic conductivity in the downstream direction represent situations which cause the minimum and the maximum equilibrium discharge among the 50 systems. As a result, V^* reaches a constant value for large T^* when K^* is high. This reasoning is in agreement with the findings of *Hawkins and Cundy* [1987], who examined extreme cases of increasing and decreasing infiltration capacity over a one-dimensional plane.

Additionally, for $T^* = T_p^*$, some of the distributed simulations did produce surface runoff. This occurs because the calculated equivalent ponding time t_p is merely based on the mean value of hydraulic conductivity. Thus, for rainfall durations equal to the equivalent ponding time, some of the grid elements with K less than K_m reach ponding before t_p. An outflow hydrograph is generated in this case when the region of the watershed near the outlet is occupied by regions with hydraulic conductivity below the mean value.

3.4. Relative Spatial Sensitivity

Relative spatial sensitivity was employed to examine the influence of the input coefficient of variation of saturated hydraulic conductivity. By defining the relative spatial sensitivity R_s as the ratio of variation in output per unit variation of spatially varied input data, one obtains

$$R_s(T^*) = \frac{V^*(T^*)}{C_v} \tag{10}$$

Figure 4 illustrates the variation of R_s versus T^* with $S = 10\%$ for two different values of K^*, 0.4 and 0.6. Generally, it

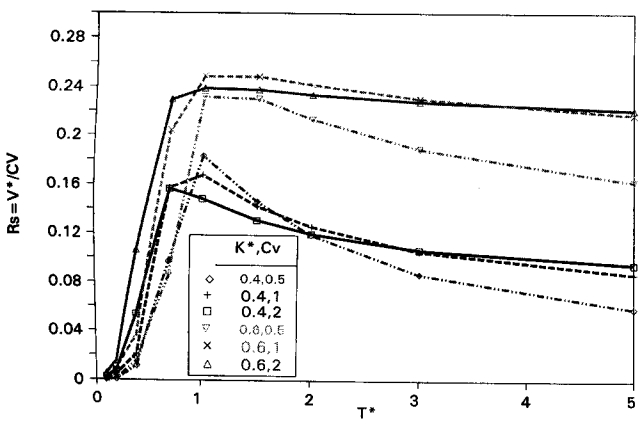

Figure 4. Relative spatial sensitivity R_s versus T^* with infiltration for $K^* = 0.4$ and 0.6.

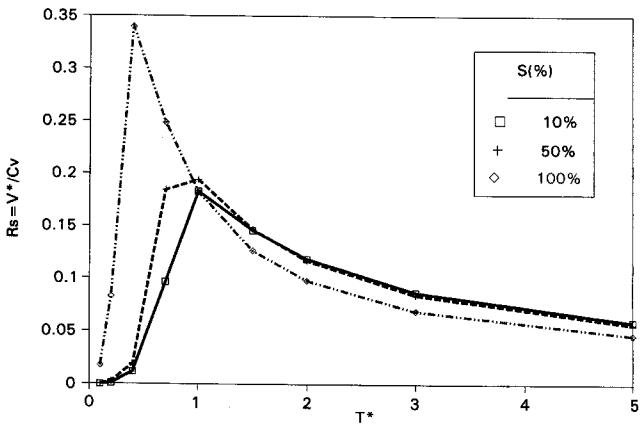

Figure 5. Relative spatial sensitivity R_s versus T^* as a function of S for $K^* = 0.4$.

can be inferred from Figure 4 that R_s is nearly insensitive to C_v, particularly for midrange values of T^*. The normalized integrated volume of the hydrograph envelope, V^*, thus varies approximately linearly in relation to the coefficient of variation of input C_v under the range of values examined in this study.

The effects of initial soil saturation S combined with spatially distributed hydraulic conductivity are collectively reported by *Saghafian* [1992]. Typical relative sensitivity versus T^* curves are shown in Figure 5 for only $C_v = 0.5$ and $K^* = 0.4$ as an example. While the relative sensitivity R_s increases with S for partial equilibrium conditions, as illustrated in Figure 4, the analysis of various values of K^* tested indicates that the effect of S on R_s becomes negligible as K^* is increased. For higher degrees of saturation, ponding occurs earlier, causing the relative sensitivity to initiate at smaller T^*. Although the antecedent soil moisture condition prior to a storm may rarely be fully saturated, spatial variability of saturated hydraulic conductivity would exert a greater influence on surface runoff for partial equilibrium hydrographs.

We now define the normalized relative sensitivity R_s^* as $R_s(T^*)/R_s(T^* = 1)$. The magnitude of the relative sensitivity R_s of runoff depends upon basin and rainfall characteristics under study and is clearly affected by which parameter is distributed spatially. However, the normalized relative spatial sensitivity may be used to strip away the effect of such characteristics to isolate the influence of a particular spatially variable parameter. Hydrologic similarity between the behavior of an impervious watershed subject to distributed rainfall [*Ogden and Julien*, 1993] and a spatially variable dry pervious watershed subject to uniform rainfall (this study) is shown in Figure 6. In the figure the normalized relative sensitivity versus T^* for various values of K^* is plotted. While R_s^* varies as a function of K^*, it asymptotically reaches the impervious case as K^* approaches zero. For short-duration rainfall events the variability of surface runoff is small prior to the time of ponding. For long-duration rainfall events, however, the effect of spatial variability of pervious watersheds on the volume of the hydrograph envelope increases with K^*. With respect to the similarity in the effect of spatial variability on surface runoff, distributed rainfall is analogous to the spatially variable dry soil when K^* is small and T^* is considerably larger than the ponding time of the mean system. With ponding occurring earlier, such similarity may be applicable in lower ranges of T^* when the initial soil condition is moist or saturated.

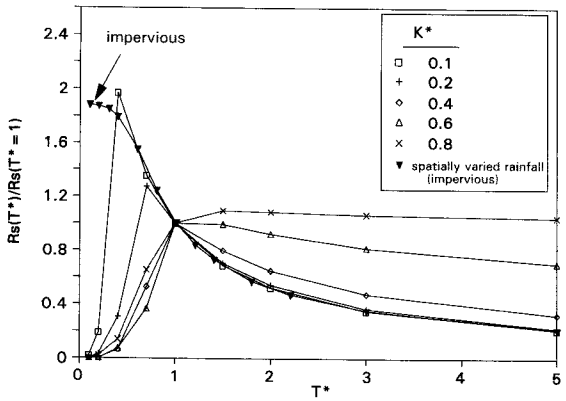

Figure 6. Normalized relative sensitivity versus T^* for pervious basins (S = 10%, C_v = 0.5) and spatially varied rainfall on impervious Macks Creek.

4. Discussions and Conclusions

The Monte Carlo analysis of the effects of spatial variability of saturated hydraulic conductivity on Hortonian surface runoff generated under stationary uniform rainfall reveals the importance of the following dimensionless governing variables: (1) the ratio of rainfall duration to the representative equilibrium time of the mean system, i.e., $T^* = t_r/t_{re}$; (2) the ratio of mean saturated hydraulic conductivity K_m to the uniform rainfall intensity, i.e., $K^* = K_m/i$; and (3) the coefficient of variation C_v of spatially distributed input data. As the rainfall duration and intensity are considered in t_{re} and K^*, it is stressed that the hydrologic behavior of spatially variable pervious watersheds depends not only on the spatial statistics of the basin characteristics, such as the mean and the coefficient of variation of the saturated hydraulic conductivity, but also on the rainfall rate and duration. In the context of hydrologic response of distributed watersheds subject to stationary rainstorms, one must note that the equilibrium time used in T^* incorporates many watershed characteristics including scale, slope, surface roughness, and geometry (convergence and divergence). The following specific conclusions are drawn based on the findings of this study:

1. Both the peak discharge and outflow volume from various systems of spatially variable hydraulic conductivity tend to be more uniformly distributed when K^* decreases and/or T^* increases.

2. The time-integrated volume within the hydrograph envelope, which is formed by the maximum and minimum discharge observed at each computational time step over a Monte Carlo ensemble of distributed systems, is most sensitive to low-intensity and long-duration rainfall (large K^* and T^*). Under these conditions the discharge produced at steady state is still dependent upon the spatial pattern of hydraulic conductivity over the watershed. This is true even for very long duration storms capable of forcing the system to virtual equilibrium conditions. This dependence is mainly attributed to the difference in the volume of run-on which infiltrates while flowing downhill.

3. The volume of hydrograph envelopes and thus the sensitivity of surface runoff hydrographs vary approximately linearly with the coefficient of variation of spatially varied hydraulic conductivity, particularly for near the center of the range of T^* values tested.

4. Most heterogeneous systems of hydraulic conductivity produce greater peak surface runoff compared to those with uniform values; this is always the case for small K^* and large T^*. Thus underestimation error in runoff discharge will likely arise when one attempts to use a uniform hydraulic conductivity while representing a spatially varied watershed. This was also pointed out by *Freeze* [1980] and by *Smith and Hebbert* [1979] at the hillslope scale. The magnitude of error will depend on T^* and K^*. These results regarding the trend in peak discharge appear to contradict the findings for high-intensity storms of *Woolhiser and Goodrich* [1988], who concluded that peak discharge was always higher for the uniform system. The discrepancy may be attributed to the use of the geometric mean in their study, while this study represented the hydraulic conductivity of the uniform system by the arithmetic mean.

5. The results of this study reveal a generally similar trend in runoff volume to the study by *Milly and Eagleson* [1988], who observed increased surface runoff volume due to spatial variability of rainfall. In this sense, as they suggested as well, the effect of spatial variability of rainfall and that of soil on runoff volume is similar, especially for small K^* and large T^*.

6. Increasing initial soil moisture contents, particularly near saturated conditions, generally causes more diversity in the hydrograph response of heterogeneous pervious watersheds excited by short-duration storms but has minimal effect under long-duration storms.

7. Characterized by the relative spatial sensitivity, similarity in the runoff response of watersheds with spatially variable soil subject to uniform rainfall (this study) and impervious watersheds subject to spatially distributed rainfall [*Ogden and Julien*, 1993] is observed in Figure 6. Such similarity, however, is limited to intense storms (low K^*). This similarity diminishes for low-intensity storms (high K^*) independent of T^*.

In summary, this Monte Carlo analysis of stationary, uniform rainstorms over a watershed with spatially variable hydraulic conductivity using a two-dimensional hydrodynamic watershed model indicates that the influence of spatial variability on peak discharge and runoff volume for pervious basins is greatest when basin-storm properties allow T^* to decrease and/or K^* to increase. By thoroughly considering the definitions of T^* and K^*, the implications are that runoff sensitivity to spatially varied infiltration increases if any of the following basin physical parameters increases: average surface roughness (in t_{re}), basin scale (in t_{re}), and average hydraulic conductivity (in K_m); and/or any of these basin-storm parameters decrease: average basin slope (in t_{re}), rainfall duration (in t_r), and rainfall intensity (in K^*).

References

Agiralioglu, N., Effect of catchment geometry on time of concentration, paper presented at 3rd International Conference on Urban Storm Drainage, Int. Assoc. for Hydraul. Res., Goteburg, Sweden, June 4–8, 1984.

Agiralioglu, N., Estimation of the time of concentration for diverging surfaces, *J. Hydrol. Sci.*, *33*(2), 173–179, 1988.

Doe, W. W., and B. Saghafian, Spatial and temporal effects of army maneuvers on watershed response: The integration of GRASS and a 2-D hydrologic model, in Proceedings, 7th Annual GRASS Users Conference, *Tech. Rep. NPS/NRG15D/NRTR-93/13*, pp. 91–165, Natl. Park Serv., Lakewood, Colo., 1992.

Freeze, R. A., A stochastic-conceptual analysis of rainfall-runoff processes on a hillslope, *Water Resour. Res.*, *16*(2), 391–408, 1980.

Hawkins, R. H., and T. W. Cundy, Steady-state analysis of infiltration and overland flow for spatially-varied hillslopes, *Water Resour. Bull.*, *23*(2), 251–256, 1987.

Henderson, F. M., and R. A. Wooding, Overland flow and groundwater flow from a steady rainfall of finite duration, *J. Geophys. Res.*, *69*(8), 1531–1540, 1964.

Johnson, B. E., N. K. Raphelt, and J. C. Willis, Verification of hydrologic modeling systems, in Proceedings, Federal Water Agency Workshop on Hydrologic Modeling Demands for the 90's, *U.S. Geol. Surv. Water Resour. Invest.*, *93-4018*, sect. 8, 9–20, 1993.

Julien, P. Y., and G. E. Moglen, Similarity and length scale for spatially varied overland flow, *Water Resour. Res.*, *26*(8), 1819–1832, 1990.

Julien, P. Y., and B. Saghafian, A two-dimensional watershed rainfall-runoff model, *Eng. Rep. CER90-91PYJ-BS-12*, Dep. of Civ. Eng., Colo. State Univ., Fort Collins, 1991.

Lighthill, M. J., and G. B. Whitham, Kinematic waves, 1, *Proc. R. Soc. London A*, *229*, 281–316, 1955.

Loague, K., and G. A. Gander, R-5 revisited, 1, Spatial variability of infiltration on a small rangeland catchment, *Water Resour. Res.*, *26*(5), 957–971, 1990.

Milly, P. C. D., and P. S. Eagleson, Infiltration and evaporation at inhomogeneous land surfaces, *Tech. Rep. 278*, Ralph M. Parsons Lab., Dep. of Civ. Eng., Mass. Inst. of Technol., Cambridge, 1982.

Milly, P. C. D., and P. S. Eagleson, Effect of storm scale on surface runoff volume, *Water Resour. Res.*, *24*(4), 620–624, 1988.

Nielsen, D. R., J. W. Biggar, and K. T. Erh, Spatial variability of field-measured soil-water properties, *Hilgardia*, *42*, 215–259, 1973.

Ogden, F. L., and P. Y. Julien, Runoff sensitivity to rainfall temporal and spatial variability at runoff plane and small basin scales, *Water Resour. Res.*, *29*(8), 2589–2597, 1993.

Ogden, F. L., and P. Y. Julien, Runoff sensitivity to radar rainfall resolution, *J. Hydrol.*, *158*, 1–18, 1994.

Rawls, W. J., D. L. Brakensiek, and N. Miller, Green-Ampt infiltration parameters from soils data, *J. Hydraul. Eng.*, *109*(1), 62–70, 1983.

Robins, J. S., L. L. Kelly, and W. R. Haman, Reynolds Creek in southwest Idaho: An outdoor hydrological laboratory, *Water Resour. Res.*, *1*(3), 407–413, 1965.

Saghafian, B., Hydrologic analysis of watershed response to spatially-varied infiltration, Ph.D. dissertation, Dep. of Civ. Eng., Colo. State Univ., Fort Collins, 1992.

Sharma, M. L., R. J. W. Barron, and M. S. Fernie, Areal distribution of infiltration parameters and some soil physical properties in lateritic catchments, *J. Hydrol.*, *94*, 109–127, 1987.

Sharma, M. L., G. A. Gander, and G. C. Hunt, Spatial variability of infiltration in a watershed, *J. Hydrol.*, *45*, 101–122, 1980.

Sivapalan, M., and E. F. Wood, Spatial heterogeneity and scale in the infiltration response of catchments, in *Scale Problems in Hydrology*, pp. 81–106, D. Reidel, Norwell, Mass., 1986.

Smith, R. E., and R. H. B. Hebbert, A Monte Carlo analysis of the hydrologic effects of spatial variability of infiltration, *Water Resour. Res.*, *15*(2), 419–429, 1979.

Wooding, R. A., A hydraulic model for the catchment-stream problem, I, Kinematic-wave theory, *J. Hydrol.*, *3*, 254–267, 1965.

Woolhiser, D. A., and D. C. Goodrich, Effect of storm rainfall intensity patterns on surface runoff, *J. Hydrol.*, *102*, 335–354, 1988.

P. Y. Julien and B. Saghafian, Civil Engineering Department, Colorado State University, Fort Collins, CO 80523.

F. L. Ogden, Department of Civil Engineering, University of Connecticut, Storrs, CT 06269.

(Received October 6, 1994; revised February 2, 1995;
accepted February 8, 1995.)